

Applied Mathematics and Nonlinear Sciences

<https://www.sciendo.com>

Research on hydrogen fuel cell backup power for metal hydride hydrogen storage system

Hang Zhang¹, Jun Pan¹, Jinyong Lei¹, Keying Feng¹, Tianbao Ma^{2,†}

1. Guangzhou Power Supply Bureau, Guangdong Power Grid Co., Ltd., Guangzhou, Guangdong, 510620, China.
2. Beijing Huasun Information Security Electronic Technology Co., Ltd., Beijing, 100089, China.

Submission Info

Communicated by Z. Sabir
 Received December 11, 2023
 Accepted December 17, 2023
 Available online January 31, 2024

Abstract

Hydrogen fuel cells are characterized by non-pollution, high efficiency and long power supply time, and they are increasingly used as backup power systems in substations, communication base stations and other fields. In this paper, based on the thermodynamic model of the hydride hydrogen storage system, the relationship between pressure, composition, and temperature in metal hydride hydrogen storage is quantitatively analyzed using a PCT curve. The hydrogen fuel power supply is used as the overall backup power supply of the DC system, and the hydrogen-fuel integrated backup power supply is established to realize the uninterrupted switching between the utility power and the backup power supply. Finally, the working process of the backup power supply and the reaction process of hydrogen are analyzed to test the feasibility of a hydrogen fuel cell backup power supply. The results show that the operating current climbs to the end of 80 A under the 5 kW workload demand of the communication equipment. In addition, the hydrogen absorption reaction rate was 0.29 Mpa, and the hydrogen release reaction rate was 0.21 Mpa at a temperature of 291 K. This study has developed a fuel cell backup power system that can provide uninterruptible backup power and has a wide market capacity and application prospects.

Keywords: Hydrogen fuel cell; Thermodynamic modeling; PCT curve; Backup power; Metal hydride.
AMS 2010 codes: 08A02

†Corresponding author.

Email address: bally287317@163.com

ISSN 2444-8656



<https://doi.org/10.2478/amns-2024-0027>



© 2023 Hang Zhang, Jun Pan, Jinyong Lei, Keying Feng and Tianbao Ma, published by Sciendo.



This work is licensed under the Creative Commons Attribution alone 4.0 License.

1 Introduction

At present, with the increase of base stations and the expansion of network scale, it not only provides users with faster and better mobile data services but also makes the energy consumption of mobile communication networks increase significantly [1-3]. At the same time, mobile communication base stations mostly use lead-acid battery packs as a backup power source, and there are also problems such as chemical pollution [4]. In the context of the “Twelfth Five-Year Plan” which requires energy saving and consumption reduction in the communication industry, the three major operators must use new energy sources in order to fulfill the energy saving and consumption reduction targets issued by the state and the operators have begun the research and construction of various new energy sources for communication base stations [5-7]. At present, the Communications Standards Committee of the Ministry of Industry and Information Technology is organizing the drafting of national standards for hydrogen fuel cells for communications and deploying and planning for hydrogen energy power supply systems for communications from the perspective of national strategy [8]. The oxygen fuel cell power supply system's widespread application in base stations is hindered by its relatively high equipment cost.

Schorn, F et al. proposed a new biogas oxyfuel process that combines a biogas plant with Power to Fuel production and enables a decentralized and economical supply of biogenic carbon dioxide for the production of renewable methanol and allows for simple separation CO_2 from flue gas by using oxygen by-products of power-to-fuel synthesis in oxyfuel combustion in a cogeneration unit [9]. Li, C evaluated the feasibility of a new energy hybrid power system using the Renewable Power Hybrid Optimization Model (RPHOM) software and employed HOMER to determine the optimal distribution size and techno-economic feasibility of the system equipment [10]. Mostafavi, S. A et al. improved the use of optimization algorithms to optimize parameters such as porosity and diameter, initial temperature and melting temperature in hydride tanks, significantly improved the hydrogen-to-metal ratio and shortened the reaction time of hydride [11].

A techno-economic evaluation of a hybrid co-generation system using hydrogen as fuel based on renewable storage technology was performed by Sofia Peláez-Peláez et al. The proposed system consists of three subsystems photovoltaic system, which generates electricity through solar energy. Hydrogen generation, consumption and storage system where an electrolyzer can be used to obtain hydrogen from water, a fuel cell that will generate electrical and thermal energy and a hydrogen tank to store hydrogen [12]. Zhu, D et al. investigated the state of charge (SOC) estimation of embedded MH hydrogen storage tanks, designed a joint multiclassifier to identify the current state of the hydrogen reaction, and indicated that at ambient temperature and pressure, metal hydride (MH) storage of hydrogen is one of the best solutions for future hydrogen-fueled vehicles [13]. Apostolou, D. found that metal hydride storage has an advantage in the price of dispensing hydrogen fuel and is expected to be a primary means of storing hydrogen for small hydrogen-fueled vehicles through a comparison between metal hydride storage devices and compressed hydrogen storage tanks [14].

Garrigos, A et al. proposed a DC/DC converter between a fuel cell standalone power supply and a hydrogen fuel backup battery, which is based on a boost topology that reduces the output filter capacitance and facilitates module parallelization and power loss management [15]. Mansir, I. B et al. modeled the transient behavior of hydrogen fuel cells and conventional battery systems using TRNSYS software, and they found that at high loads, the use of hydrogen fuel cells has better performance, but the capital cost of the hydrogen fuel cell system is twice as much as the cost of the conventional battery system [16]. Bedrunka, M et al. used numerical simulation analysis to evaluate an on-board metal hydride storage system and explored the feasibility of hydrogen alloys Co_5 or FeTiMn for application of the technology on a fuel cell forklift [17].

In this paper, firstly, hydrogen storage alloy LaNi_5 is used as a hydrogen storage material, and the chemical reaction process of metal hydride is explored by reaction kinetic equation and equilibrium pressure equation. The hydrogen storage system is used to store the hydrogen required by the fuel cell by constructing a backup power supply that uses hydrogen fuel integrated with the fuel cell. The DC/DC converter unit stabilizes the variable voltage generated by the fuel cell and outputs it to the load voltage. Secondly, the working mechanism of the metal-hydrogen fuel cell backup power system is discussed, and status data is transmitted to the monitoring center through the human-machine interface. The response is based on the state of the backup power system, AC power operation, and battery SOC. The hydrogen fuel system is normal and stable operation is ensured through the use of the PI proportional-integral regulation control strategy. Finally, the feasibility of the hydrogen fuel cell backup power scheme for the metal hydride hydrogen storage system is explored by calculating the working process of the backup power and analyzing the thermodynamic characteristics of the hydrogen absorption and discharge reaction process.

2 Method

2.1 Thermodynamic modeling of hydride hydrogen storage systems

Metal hydride (MH) hydrogen storage system is one of the indispensable links to promote the application of hydrogen energy. With high volumetric hydrogen storage density, low operating pressure and good reversibility, it has a wide range of application prospects in the field of transportation, microgrid, hydrogen compression, heat storage, etc. MH hydrogen storage, a method of hydrogen storage, refers to the storage of hydrogen in the form of atoms in a metal or an intermetallic compound as a reversible reaction process. The process of absorbing hydrogen is exothermic, while the process of releasing it is absorptive. In general, the pressure-composition-temperature relationship for MH hydrogen storage can be quantitatively described by a PCT curve. At the beginning of the reaction, hydrogen is dissolved into the host metal to form a α -phase solid solution. As the solid solution content increases, a β -phase metal hydride begins to form.

2.1.1 Mass conservation equations

In this study, hydrogen storage alloy LaNi_5 is used as a hydrogen storage material for a metal hydride hydrogen storage system. Its hydrogenation-dehydrogenation reaction equation can be expressed as $\text{LaNi}_5 + 3\text{H}_2 \leftrightarrow \text{LaNi}_5\text{H}_6 + \Delta H$, where ΔH represents the heat of the reaction. In general, gaseous hydrogen and solid materials are present inside a metal hydride hydrogen storage tank. The solids in the tank include the hydrogen storage alloy LaNi_5 and the metal hydride LaNi_5H_6 . The relationship between the mass of the solids and the mass of the hydrogen storage alloy, and the mass of the metal hydride in the hydrogen storage tank can be expressed as follows:

$$m_s = m_M + m_{\text{MH}} \quad (1)$$

During hydrogenation, the hydrogen storage alloy reacts with hydrogen to form a metal hydride, with a mass m_M of the hydrogen storage alloy gradually decreasing and the mass m_{MH} of the metal hydride gradually increasing. During dehydrogenation, in contrast, the metal hydride decomposes into the hydrogen storage alloy and hydrogen, with the mass m_M of the hydrogen storage alloy gradually increasing and the mass m_{MH} of the metal hydride gradually decreasing. Overall, solid

mass m_s gradually increases during hydrogenation, and solid mass m_s gradually decreases during dehydrogenation.

The saturation mass of the solids is given as m_s^{sat} . When all of the hydrogen storage alloy in the system has reacted with hydrogen to produce the metal hydride, the mass of the metal hydride reaches a maximum value of $m_{\text{MH}}^{\text{max}}$. The relationship between the two species is given by:

$$m_s^{\text{sat}} = 0 + m_{\text{MH}}^{\text{max}} \quad (2)$$

The solid mass m_s can be written as the sum of the initial mass ($m_{0\text{M}} + m_{0\text{H}}$) in the hydrogen storage tank and the mass m_{H} of elemental hydrogen added to the tank by the later hydrogenation reaction:

$$m_s = m_{0\text{M}} + m_{0\text{H}} + m_{\text{H}} \quad (3)$$

Where $m_{0\text{M}}$ and $m_{0\text{H}}$ represent the mass of the hydrogen storage alloy in the initial state and the mass of absorbed hydrogen in the initial state, respectively. When there is only the hydrogen storage alloy in the hydrogen storage tank in the initial state, the mass $m_{0\text{H}}$ of the absorbed elemental hydrogen is 0 at this time.

The saturation mass m_s^{sat} of a solid substance can be expressed as the sum of the mass $m_{0\text{M}}$ of the initial hydrogen storage alloy and the mass $m_{\text{H}}^{\text{max}}$ of the maximum amount of elemental hydrogen that can be absorbed by the hydrogen storage system, which can be expressed as:

$$m_s^{\text{sat}} = m_{0\text{M}} + m_{\text{H}}^{\text{max}} \quad (4)$$

The relationship between the mass m_{H} of absorbed elemental hydrogen and the mass m_{MH} of the metal hydride can be expressed as:

$$m_{\text{H}} = m_{\text{MH}} \psi M_{\text{H}_2} / M_{\text{MH}} \quad (5)$$

Where the letter ψ is defined as the stoichiometric coefficient of hydrogen per unit of metal hydride, and M_{MH} M_{H_2} denote the molar molecular weights of the metal hydride and hydrogen, respectively.

For the lumped parameter model, the generalized form of the mass conservation equation can be expressed as:

$$\frac{dm}{dt} = \dot{m} + \dot{S} \quad (6)$$

Where \dot{m} denotes the net mass flow rate and \dot{S} denotes the net mass generation rate or mass source term. This mass conservation equation in a metal hydride hydrogen storage system can be applied to the metal hydride in the tank, the gas-phase hydrogen, and the solids, respectively, and can be expressed as:

$$\frac{dm_{MH}}{dt} = \dot{S}_{MH} \quad (7)$$

$$\frac{dm_{H_2}}{dt} = \dot{m}_{H_2} + \dot{S}_{H_2} \quad (8)$$

$$\frac{dm_s}{dt} = -\dot{S}_{H_2} \quad (9)$$

During hydrogen absorption, the metal hydride mass source term \dot{S}_{MH} is positive. During dehydrogenation, the metal hydride mass source term \dot{S}_{MH} is negative. For gaseous hydrogen in tanks, the hydrogen mass source term \dot{S}_{H_2} is negative during hydrogen absorption. During dehydrogenation, the hydrogen mass source term \dot{S}_{H_2} is positive. The hydrogen mass flow rate \dot{m}_{H_2} is equal to the difference between the inflow mass flow rate $\dot{m}_{H_2,in}$ and the outflow mass flow rate $\dot{m}_{H_2,out}$, with the subscripts in/out indicating the inflow and outflow states, respectively. In hydrogen absorption, the outflow mass flow rate is assumed to be 0, i.e., $\dot{m}_{H_2,out} = 0$. In dehydrogenation, the inflow mass flow rate is assumed to be 0, i.e., $\dot{m}_{H_2,in} = 0$.

The relationship between the metal hydride mass source term \dot{S}_{MH} and the hydrogen mass source term \dot{S}_{H_2} can be expressed as follows:

$$\dot{S}_{MH} = -\dot{S}_{H_2} M_{MH} / (\psi M_{H_2}) \quad (10)$$

The mass source term for metal hydrides is related to the kinetic equation for the reaction of metal hydrides and the equilibrium pressure equation, which are described in the next section.

2.1.2 Reaction kinetics and equilibrium pressure equations

The mass source term of the metal hydride in the hydrogen absorption or dehydrogenation phase, respectively, can be expressed as:

$$\dot{S}_{MH} = C_a e^{-E_a/(RT)} \ln \frac{p_{H_2}}{p_{eqa}} (m_s^{\text{sat}} - m_{MH}) \quad (11)$$

$$\dot{S}_{MH} = C_d e^{-E_d/(RT)} \frac{p_{H_2} - p_{eqd}}{p_{eqd}} m_{MH} \quad (12)$$

where m_s^{sat} denotes the saturation mass of the solid, which is numerically equal to the maximum mass of the metal hydride m_{MH}^{max} . E denotes the activation energy and the subscripts a/d denote the hydrogen uptake/dehydrogenation process, respectively. During hydrogen absorption, the hydrogen pressure p_{H_2} is greater than the equilibrium pressure p_{eqa} , i.e., $p_{H_2} > p_{eqa}$. During dehydrogenation, the hydrogen pressure p_{H_2} is less than the equilibrium pressure p_{eqd} , i.e.,

$p_{H_2} < p_{eqd}$. When the hydrogen pressure p_{H_2} is located between p_{eqa} and p_{eqd} , the mass source term of the metal hydride, \dot{S}_{MH} , is set to zero.

The equilibrium pressure $p_{eqa/d}$ of the metal hydride hydrogen storage system can be expressed as:

$$\ln \frac{p_{eqa/d}}{p_0} = -\frac{\Delta H_{a/d}}{RT} + \frac{\Delta S_{a/d}}{R} + k_p \left(\frac{m_{MH}}{m_s^{sat}} - \frac{1}{2} \right) \quad (13)$$

Where the reference pressure p_0 is set to 0.1 MPa. In this paper, the reaction enthalpy ΔH and reaction entropy ΔS are both set to positive numbers, and the symbol k_p denotes the slope coefficient.

2.1.3 The energy conservation equation

Heat exchangers can improve heat transfer inside metal hydride hydrogen storage tanks, but they can also complicate the overall hydrogen storage system. For simplicity, heat exchangers are not considered for hydrogen storage systems in this chapter, and the effect of hydrogen storage tank walls is ignored. The energy conservation systems equation for the metal hydride hydrogen storage system can be expressed as:

$$\frac{d(m_{H_2} c_v T + m_s c_s T)}{dt} = \dot{m}_{H_2} c_p T_\infty + a_f A_s (T_f - T) - \frac{\dot{S}_{H_2} \Delta H_{a/d}}{M_{H_2}} \quad (14)$$

Where m_{H_2} indicates the mass of gaseous hydrogen in the hydrogen storage tank, c_s indicates the specific heat capacity of the solid phase substance, T_∞ indicates the filling or deflating temperature, a_f indicates the heat transfer coefficient, A_s indicates the surface area of the hydrogen storage tank and T_f indicates the ambient temperature. When external circulating water is used to cool or heat the hydrogen storage tank, the temperature of the circulating water can be set to the ambient temperature. The part to the left of the equal sign in Eq. (14) represents the rate of change of internal energy of the metal hydride hydrogen storage tank. Based on Eq. (8) and Eq. (9), the part D to the left of the equal sign of Eq. (14) can be transformed:

$$D = (m_{H_2} c_v + m_s c_s) dT / dt + c_v T (\dot{m}_{H_2} + \dot{S}_{H_2}) - c_s T \dot{S}_{H_2} \quad (15)$$

It can be seen that during hydrogen absorption, the energy source term is positive. During dehydration, the energy source term is negative. As discussed earlier, the energy conservation equation for the metal hydride hydrogen storage system can be transformed into:

$$\begin{aligned} & (m_{H_2} c_v + m_s c_s) \frac{dT}{dt} = \\ & \dot{m}_{H_2} (c_p T_\infty - c_v T) + a_f A_s (T_f - T) - \dot{S}_{H_2} [(c_v - c_s) T + \Delta H_{a/d} / M_{H_2}] \end{aligned} \quad (16)$$

2.1.4 Ideal gas equation of state

In a metal hydride hydrogen storage system, hydrogen is considered an ideal gas, and its gas equation of state is expressed as:

$$m_{H_2} = \frac{p_{H_2} V_g M_{H_2}}{RT} \quad (17)$$

Where p_{H_2} denotes the hydrogen pressure, V_g denotes the volume of gaseous hydrogen in the hydrogen storage tank, and R denotes the universal gas constant, which has a value of 8.315 J/mol/K.

2.2 Hydrogen-fueled integrated backup power

The conversion of chemical energy of hydrogen and oxygen into electrical energy is directly done by hydrogen fuel cells, which are highly efficient electrochemical energy converters. As long as there is a constant input of fuel and air, the fuel cell can continuously generate electrical energy. Therefore, the fuel cell has the characteristics of both a battery and an oil engine. The working principle of the hydrogen fuel cell is shown in Fig. 1, and the interior of the fuel cell is mainly composed of a proton exchange membrane, electrochemical reaction catalyst, diffusion layer and bipolar plates [18].

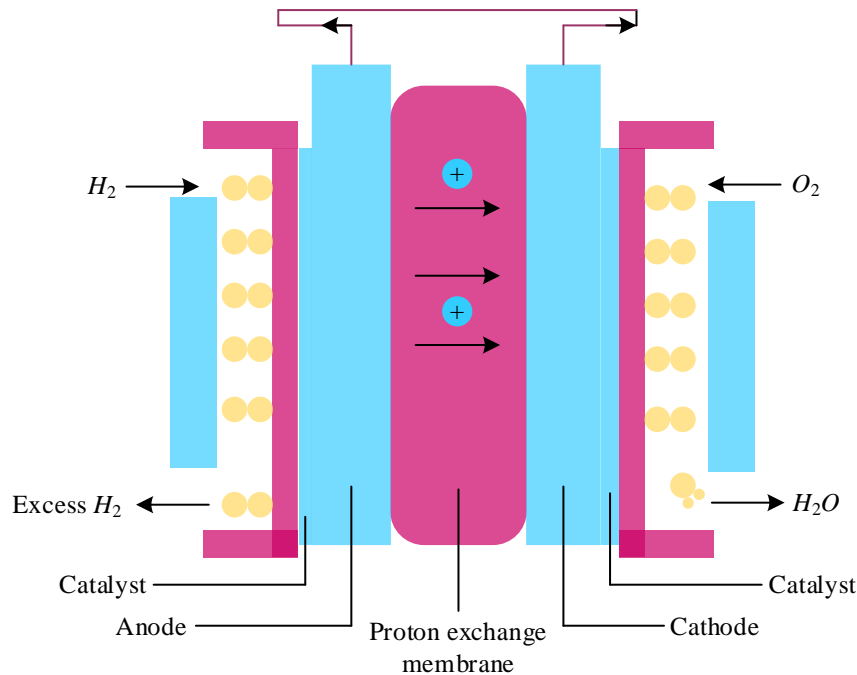


Figure 1. Working principle of hydrogen fuel cell

When a fuel cell operates, the following reaction process occurs within it:

The anode (negative electrode) is:



The cathode (positive) is:



The battery reaction is:



The reactive gas diffuses within the diffusion layer, and when the reactive gas reaches the catalytic layer, it is adsorbed by the catalyst within the catalytic layer and undergoes an electrocatalytic reaction. The protons generated from the anode reaction are transferred to the cathode side through the proton exchange membrane inside, and the electrons reach the cathode through the external circuit, reacting and combining with the oxygen molecules to form water and releasing heat at the same time.

The hydrogen fuel integrated backup power supply realizes a complete set of hydrogen fuel cell backup power supply systems with a power of 5 kW, which includes a hydrogen storage system, a hydrogen fuel cell system, a DC/DC converter system, a monitoring system, a UPS, a lithium battery and so on, and the principle of the system is shown in Figure 2. The hydrogen storage system is used to store the hydrogen required by the fuel cell, and the chemical reaction between hydrogen and oxygen occurs in the fuel cell system to generate electrical energy. The DC/DC converter unit stabilizes the fuel cell's variable voltage output to meet the load's voltage requirements. The monitoring unit is used for signal acquisition, DC/DC output management, fuel cell control, motor control, alarm, battery protection, communication interface, automatic start, manual start, remote start and other monitoring functions.

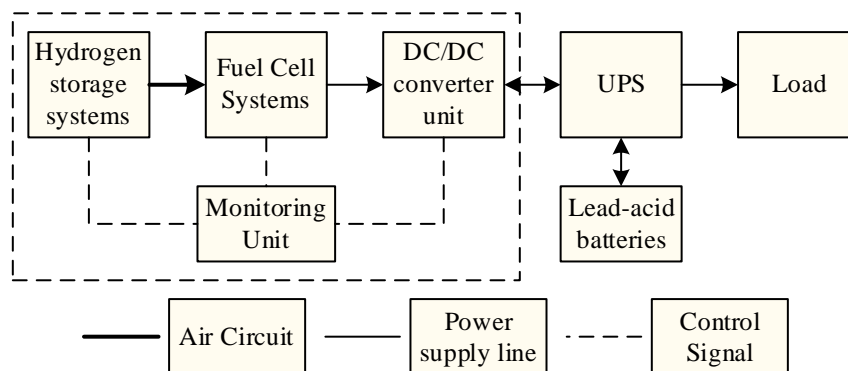


Figure 2. Principle of hydrogen fuel integrated backup power supply system

When the backup power system detects that the bus voltage is consistently below 120V for 5 seconds, it will start the fuel cell for the power supply. The DC/DC has a slow-start function, which achieves the purpose of slow-start by gradually releasing the output current. When the current required by the load is greater than the current output from DC/DC, the voltage of DC/DC will automatically drop to the same level as the UPS battery, so the UPS will also output part of the current to meet the needs of the load. When the output current of DC/DC meets the requirement of load, the output voltage of DC/DC will be restored to the set value, and at the same time, the UPS battery does not output current externally. When the utility power is restored, the equipment system stops the power supply and enters standby mode. At the same time, the UPS battery is charged through the UPS internal switching power supply, and the float voltage is 60V.

2.3 Working Mechanism of Metal Hydrogen Fuel Cell Backup Power System

2.3.1 Mechanism of operation of the backup power supply

When the metal-hydrogen fuel cell is used as an independent power supply, it is difficult to meet the requirements of the load voltage level, so it is necessary to meet the load requirements through the power amplifier. The framework of the metal-hydrogen fuel cell backup power system is shown in Fig. 3, which can realize the characteristic of supplying power to DC loads, but also monitor the power supply status of AC power source and the operation status of the backup power system itself in real-time after the system starts. And through the human-computer interface and monitoring center for status data transmission. The system control unit reacts in accordance with the state of the backup power system, the AC power supply's operating status, and the lithium battery's SOC.

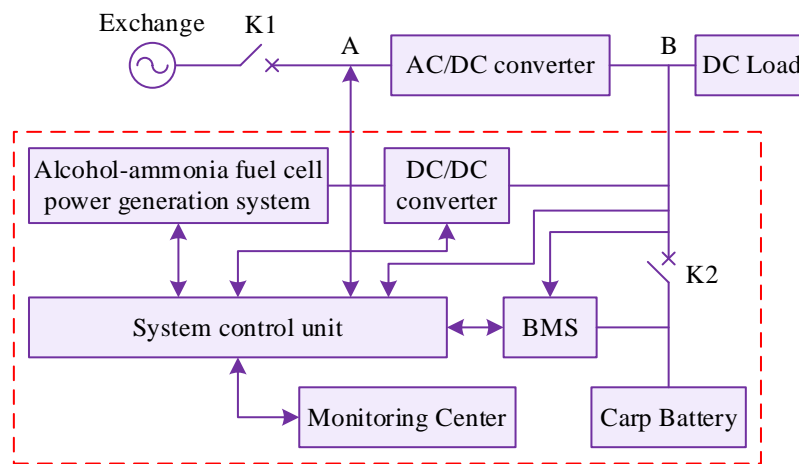


Figure 3. Block diagram of metal hydrogen fuel cell backup system

When the entire backup power system completes the preparatory work, close switch K1 through the inverter device for the DC equipment power supply. At the same time, the hydrogen fuel cell backup power system enters the start state, closes switch K2, and access to lithium iron phosphate battery. Hydrogen fuel cell backup power system, a variety of power supply state conversion schematic shown in Figure 4.

First of all, the system automatically initializes the setup state and detects whether the AC power supply state is normal. According to the detection results, to determine whether the backup power system will provide electricity, if normal, the hydrogen fuel cell backup power system will be in standby mode. Conversely, the hydrogen fuel cell starts generating electricity to continue supplying power to the DC load. Among them, the BMS subunit manages the charging of the lithium battery.

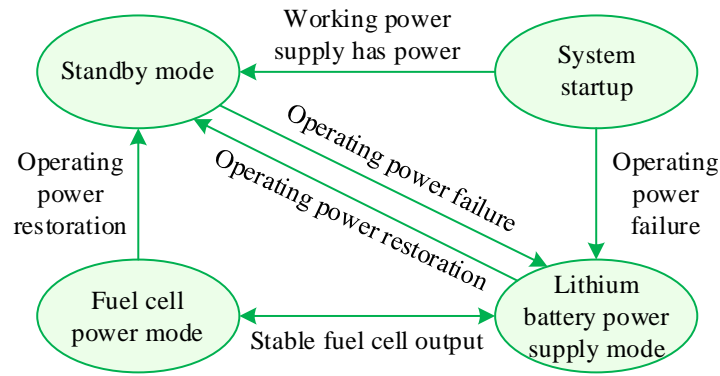


Figure 4. Switching of standby power mode of hydrogen fuel cell

The lithium battery is floating when AC mains power is functioning normally. When the system monitors the power failure, the lithium battery first enters the discharge state to provide a short-term power supply for the load at the same time but also for the start of the hydrogen fuel cell as an auxiliary power source. As the hydrogen fuel cell module starts to output power, the system enters the fuel cell power supply mode. After working for some time, if the AC power supply is monitored, the backup power system will automatically cut out and enter the standby mode, the hydrogen fuel cell enters the cool standby state, and the working power supply powers the load.

2.3.2 Standby power system operating mode

According to the above analysis of the working principle of the standby power supply system, after the system starts running, it makes an initialization judgment on the power supply type and then enters into different power supply states, and the system is divided into four working modes through detection as shown in Fig. 5.

1) Mode 1

When the AC mains power is working normally, as shown in Fig. 5(a), it can supply power to the DC loads through AC/DC inverter, the hydrogen fuel cell is in the standby state, and the lithium battery is in float charging state.

2) Mode 2

When the AC mains power is suddenly disconnected, as shown in Fig. 5(b), it directly switches into the lithium battery power supply mode, which can provide power supply for the load for a short time, and the hydrogen fuel cell enters the start-up state after detecting the set voltage signal.

3) Mode 3

When the fuel cell starts to generate power, as shown in Fig. 5(c), its initial power generation is small, so the load is powered by the lithium battery and hydrogen fuel cell together.

4) Mode 4

When the hydrogen fuel cell enters the stable power generation stage, as shown in Fig. 5(d), it acts as the main power source to supply power to the load, and it can also charge the lithium battery.

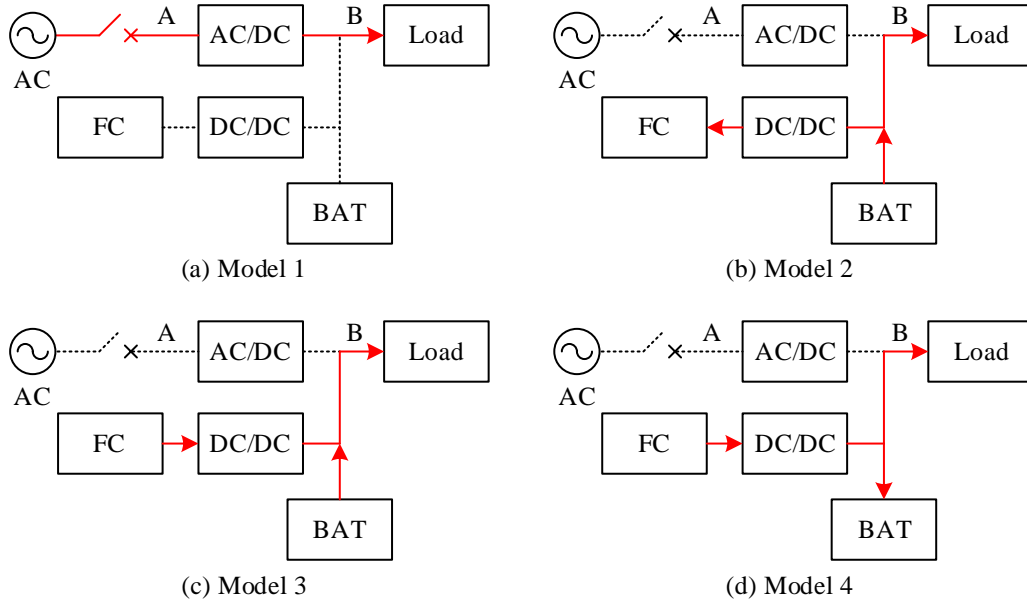


Figure 5. Standby power system working mode

2.3.3 System control strategy

The output voltage control structure of the fuel cell system is shown in Fig. 6, and the PI proportional-integral regulation control strategy is adopted to ensure the reliable, normal and stable operation of the system, with the hydrogen fuel cell as the main power source. The reference current is obtained from the ratio of the reference power to the DC bus voltage, and then compared with the command current, and the error current obtained is determined by the PI controller to control the duty cycle of the comparison output. The output of the hydrogen fuel cell module is connected to the DC bus through the power converter.

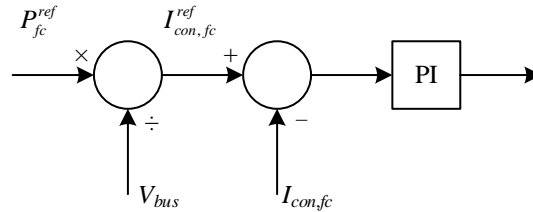


Figure 6. Output voltage control structure of the fuel cell system

3 Result and Discussion

3.1 Analysis of the working process of hydrogen fuel cell backup power supply

3.1.1 Current response analysis

In this paper, the metal-hydrogen fuel cell backup power system constructed in the previous paper is applied in the mobile base station backup power supply, and its DC management module adopts 2-stage DCDC conversion. The first stage conversion converts the DC output of the fuel cell stack into 60 V DC, and the second stage DCDC boosts the 60 V DC output of the first stage to 220 V DC to

meet the power requirements of the power substation of the power system. The hydrogen storage unit consists of hydrogen storage tanks, manifolds, control valves, etc. The hydrogen storage tanks generally use national standard metal cylinders and are placed outdoors, which helps to solve the problems of hydrogen safety and the convenience of replacing cylinders.

According to the power demand at the work site, when the power grid is suddenly cut off, the hydrogen fuel cell backup power system should be able to output 5 kW of DC power at the first time, which means that the first-stage DCDC should output about 60 A of DC power. In order to illustrate the starting process of the system and the response of the system under sudden load change, the system is first started with a 2 kW load, then the load is suddenly changed to 3 kW, and finally, the load is suddenly changed to 5 kW, and the response of the system is examined under three working conditions as shown in Fig. 7. It can be seen that the primary DCDC does not provide the required 60 A (5 kW) current at time 0 when the current is essentially all from the 50 Ah 60 V DC battery bank. Moreover, the battery bank also provides power to the system electronic control unit and auxiliary machines, i.e., the hydrogen supply unit, the oxidizer supply unit and the heat exchange unit in the fuel cell module, to maintain the power required for their startup and operation. With time, the hydrogen fuel cell system gradually completes the filling of fuel and oxidizer under the control of the system's electronic control unit, replacing the power supply of the battery. The output current of the DCDC climbs at a rate of 1 A/s from the moment of 0, and when it reaches 40 s, the battery stops supplying power, and the fuel cell system is responsible for charging the battery with a small current in addition to providing all the 5 kW of power supply, so the fuel cell system completes the startup process, and it can supply power to DC loads in a stable manner. The DCDC power comes from the stack, so you can see that the output of the stack rises synchronously.

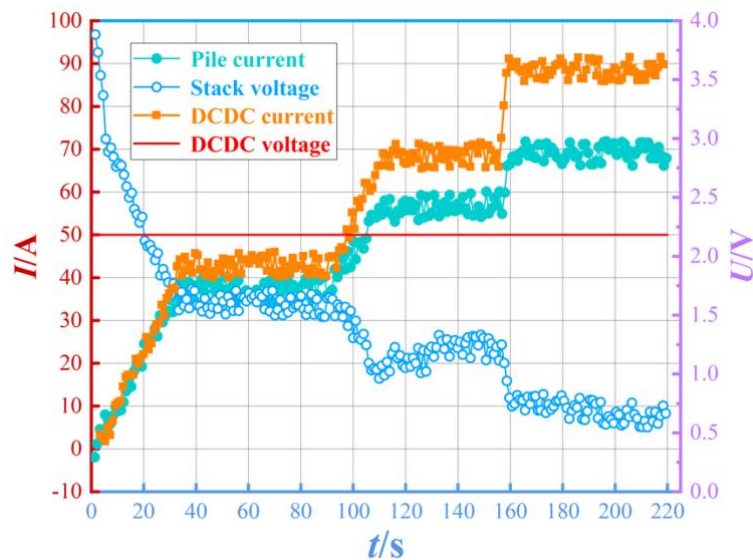


Figure 7. Startup process of fuel cell system

3.1.2 Voltage response analysis

From the current response analysis, it is known that the changes in the voltage of the electrostack and the output voltage of the first-stage DCDC during the startup process of the hydrogen fuel cell backup power supply, and the output voltage of the DCDC does not change much during the startup process because the first-stage DCDC and the 50 A battery are jointly connected to the bus. The current creep curve during the actual starting process is shown in Figure 8. It can be seen that with the gradual increase of the output current of the stack, the output voltage of the stack has a very obvious drop

from the open circuit voltage of 73 V at the moment of 0 to about 47 V at the moment of 20 s, i.e., at the end of the creepage of 80 A. Combined with Fig. 7, the voltage of the stack decreases to 45 V at a load of 2 kW, and at a load of 3 kW, the voltage decreases to about 42 V. It is noticed that the voltage of the stack is relatively high compared to the output voltage of the DCDC. The voltage fluctuations are large because of changes in control factors like hydrogen supply, oxygen supply, and electrostack temperature.

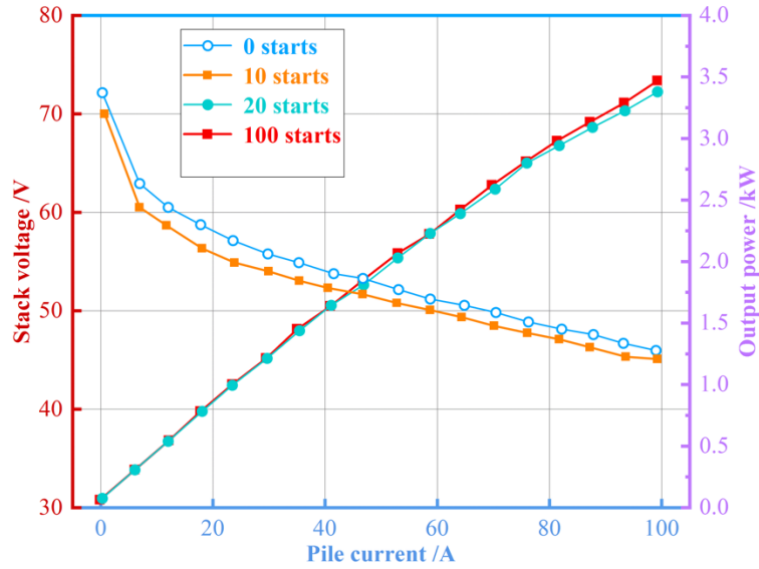


Figure 8. Current increasing curve in actual booting process

From the above discussion, it can be concluded that the hydrogen fuel cell system designed in this paper can meet the standby power demand of the substation of the electric power system, realizing the “zero-waiting” of the power supply, and can replace the lead-acid battery pack with the hydrogen fuel cell standby power.

3.2 Economic analysis of different backup power system options

The cost of acquiring the new hydrogen fuel cell backup power system is significantly more expensive than the current lead-acid battery backup power system. However, with the large-scale production of this new backup power system in the future and a series of financial subsidy measures taken by the state for green equipment, the initial acquisition cost of the new backup power system will be reduced.

In this paper, an experience curve is used to estimate the trend of the cost of the system over time and the scale of production so as to estimate the time when the cost of the equipment of the old and new systems is roughly comparable. An experience curve, also known as a learning curve, is a curve that represents the relationship between units of time produced and units of continuous production and can, therefore, be used to analyze the long-term potential of a new hydrogen fuel cell backup power system and to predict the cost of the system, thereby providing a basis for decision-making on the replacement of the old and new systems. A typical equation for the experience curve is:

$$Y_i = AX_i^{-r} \quad (21)$$

where X_i is the total amount of production when the i nd product is produced, Y_i is the cost of producing the i th product, A is usually a constant indicating the cost of producing the first product, and the exponent r is the rate of progress. When the total number of products is doubled, there is

$F = 2^{-r}$, which reflects the rate of progress in the production of the product. Empirical values for the rate of progress for certain types of products can be derived from a large amount of data, ranging from 0.8 to 0.9 for mechanically assembled products and 0.7 to 0.85 for electronic devices and semiconductors.

Based on further research and in conjunction with this paper's analysis of the initial cost of equipment under several base station energy consumption conditions, it is known that the initial cost of equipment for a system generally increases in a certain proportion based on the generation power. Therefore, the initial cost invested per unit of generating power is used here to express the initial cost of equipment purchased for the new type of system in 10,000 yuan/kW. For the new hydrogen fuel cell backup power system, its initial acquisition equipment cost is mainly composed of hydrogen fuel cell power generation unit equipment cost and hydrogen storage unit equipment cost, which is currently about 60,000 yuan/kW. For the existing lead-acid battery backup power supply system, its initial acquisition equipment cost is mainly composed of lead-acid battery component cost, which is about 12,000 yuan/kW at this stage.

Currently, the new hydrogen fuel cell backup power supply system has not been mass-produced, so it is assumed that the number of products produced doubles every year, and an empirical value of 0.8 is used as the production progress rate for the equipment of the new hydrogen fuel cell backup power supply system. Lead-acid batteries have been mass-produced for many years, and technological innovations are gradually decreasing. An empirical value of 0.9 is used to determine the production progress rate of the current backup power supply system equipment. Using the experience curve, this section projects how the cost of key equipment for the old and new systems will change over time with the scale of production over the next 20 years, using 2022 as the starting point, as shown in Figure 9. In the beginning 10 years, the equipment cost of the hydrogen fuel cell power supply system is still higher than the equipment cost of the existing power supply system, and the cost difference is about 0.5 to 48 thousand dollars/kW. As the annual production quantity increases, the equipment cost gap between them decreases each year. According to the assumption conditions in this paper, the equipment cost gap between the two is less than 10,000 yuan/kW by about 2028, i.e., the equipment cost of the hydrogen fuel cell backup power system can already be compared with that of the storage battery. As production continues to expand, the key equipment costs of the old and new systems will reach about the same level by 2034.

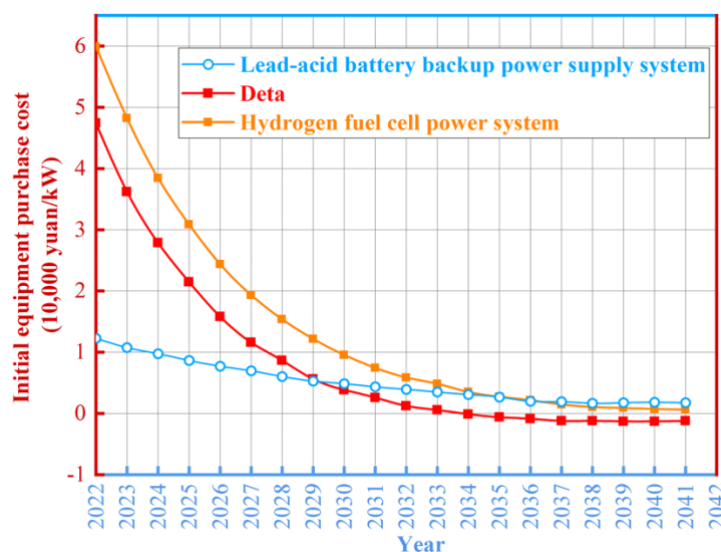


Figure 9. Empirical cost prediction curve of key equipment in old and new systems

Therefore, based on the cost projection curves in the figure (Dear), it can be deduced that the gradual replacement of the existing backup power supply system for large base stations can begin around 2029 and that the aid of government fiscal subsidies can be largely eliminated by around 2030.

3.3 Hydrogen Reaction Simulation and Test Analysis of Hydrogen Fuel

The PCT curve is an important characterization of the MH hydrogen adsorption and discharge process, which not only reflects the adsorption and desorption characteristics of the MH hydrogen storage material but also expresses the dynamic performance of the reaction process. Therefore, the acquisition of PCT curves is an important part of evaluating the performance of MH hydrogen storage tanks. Based on this, the absorption/release hydrogen reaction characteristics of hydrogen fuel are analyzed in combination with simulation tests.

3.3.1 Analysis of the hydrogen absorption process

For the absorption process, hydrogen is continuously filled into the MH hydrogen storage tank; in the initial stage, the hydrogen concentration inside the tank is low, the absorption of hydrogen by the MH is not obvious, and the structure of the hydrogen storage material is almost unchanged. With the gradual increase of hydrogen concentration, the hydrogen atom content within the hydrogen storage alloy crystals gradually increases, and the hydrogen absorption reaction is gradually accelerated to a fast and smooth process, and the pressure in the tank reaches equilibrium at this stage. At the late stage of the reaction, the MH hydrogen content tends to be saturated, the gaseous hydrogen fills up the void inside the tank, the pressure inside the tank rises rapidly, and the rate of hydrogen absorption reaction decreases gradually. The PCT curves of hydrogen absorption at different temperatures are shown in Fig. 10, which are derived from the simulation model at temperatures 291, 305 and 312 K, and from the test bench at temperature 298 K. According to the trend of the curves in the figure, it can be seen that at $H/H_{max} = 0.8$ o'clock, 291, 305 and 312 K conditions, the hydrogen absorption reaction rate is 0.29, 0.46 and 0.68Mpa, and the increase of temperature will increase the hydrogen absorption reaction rate. At the same time reduce the total hydrogen absorption of the metal hydrogen storage tank, which is not conducive to the reaction.

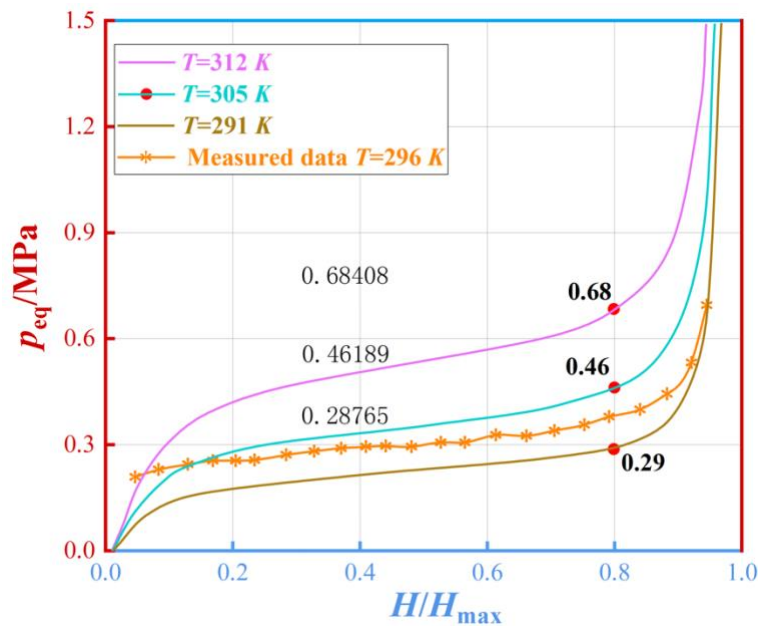


Figure 10. P-C-T curves of hydrogen absorption at different temperatures

For the dynamic process of hydrogen absorption in the MH tank, the initial temperature and circulating water inlet temperature are set to 291 K, and the initial pressure is the equilibrium pressure of hydrogen absorption at this temperature, and the change of the state of the MH tank during the reaction process is shown in Fig. 11. It can be seen that, with the continuous charging of hydrogen, the hydrogen content gradually increased until saturation, in the initial stage, the rate of hydrogen charging in the tank is greater than the rate of hydrogen absorption reaction, the hydrogen content H / H_{\max} increased rapidly, and the hydrogen absorption reaction performance tends to stabilize after 4.0×10^{-4} , and the hydrogen content continues to increase. When H / H_{\max} is greater than 0.96, the tank becomes saturated and the rate of hydrogen absorption decreases significantly until it is filled.

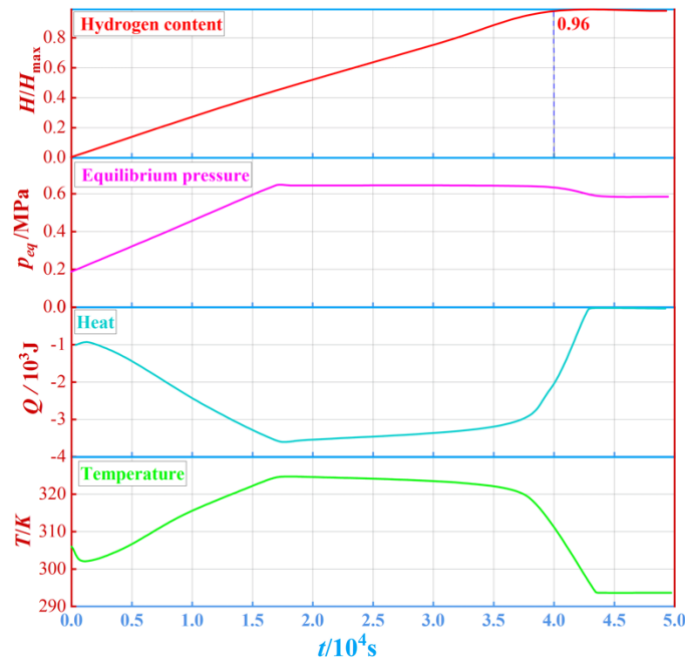


Figure 11. Basic characteristics of hydrogen absorption in hydrogen storage tank

From the equilibrium pressure curve, it can be seen that the pressure of hydrogen in the tank rises faster in the starting phase ($0-1.7 \times 10^4$ s), and the absorption of hydrogen in this phase is mainly driven by the pressure difference between the internal pressure of the hydrogen storage tank and the equilibrium pressure. When hydrogen is supplied continuously, the pressure of hydrogen inside the tank is higher than the equilibrium pressure at that temperature, which drives the absorption of hydrogen in the tank. As the hydrogen absorption reaction slows down, the hydrogen pressure remains in dynamic equilibrium with the equilibrium pressure. At this point, the value of p_{eq} / MPa is 0.605, and this stage is in the plateau period. The rate of hydrogen absorption decreases significantly at the later stage of the reaction, and the equilibrium pressure decreases under the influence of temperature until it stabilizes at about 0.598.

From the heat and temperature curves, it can be seen that the hydrogen absorption reaction releases heat to the circulating water, and in the initial stage, due to the rapid increase of the reaction rate, the circulating water absorbs a large amount of heat from the MH hydrogen storage material, which at the same time leads to a rapid increase in the temperature of the hydrogen storage tank. As the reaction gradually reaches equilibrium and slows down, the heat absorbed by the circulating water gradually decreases, and the hydrogen storage tank temperature gradually returns to room temperature of 293K.

3.3.2 Analysis of the hydrogen release process

Since the hydrogen release reaction is the inverse process of the hydrogen absorption reaction, the end state of the hydrogen absorption process can be taken as the initial state of the hydrogen release reaction at the same temperature. Figure 12 shows the PCT curves obtained from the simulation of the hydrogen release reaction model, and the three curves are the PCT curves of the hydrogen release reaction at temperatures 291, 305 and 312 K, respectively. Combined with the test data, the PCT curve at temperature 296 K can be plotted. According to the influence of temperature on the reaction rate and the amount of hydrogen release in the graph, it can be concluded that at $H/H_{max} = 0.8$ o'clock, 291, 305 and 312 K, the rate of hydrogen release reaction is 0.21, 0.32 and 0.46Mpa, which indicates that increasing the temperature is favorable for the hydrogen release reaction. Meanwhile, it can be seen that the shapes of the PCT curves of the hydrogen absorption reaction and the hydrogen release reaction are basically the same, and the difference is the height of the plateau region. The hysteresis effect causes the height of the hydrogen release platform to be lower than that of the hydrogen absorption platform. Pressure hysteresis results in a decrease in the reaction driving force, resulting in an additional decrease in the reaction rate.

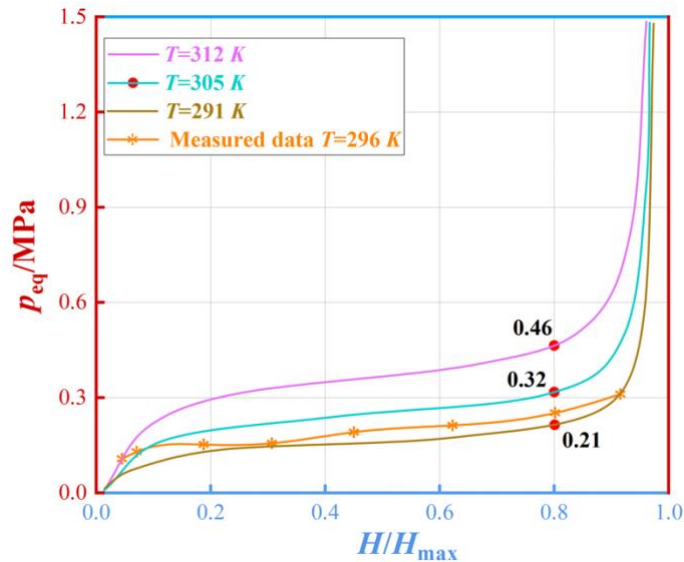


Figure 12. P-C-T curves of hydrogen emission at different temperatures

Ideally, the hydrogen absorption and discharge reaction PCT curves are flat and overlapping. However, due to the influence of local defects of the material, surface state, compositional inhomogeneity and other factors, the hydrogen absorption and discharge platform has a height difference and produces a certain degree of tilt. The simulation test and analysis of the hydrogen reaction of hydrogen fuel can provide a theoretical reference for the application and optimal control of metal hydride hydrogen storage as a backup power source.

4 Conclusion

With the rapid development of the mobile communication industry, the mobile communication network is expanding, and the energy consumption and pollution of the whole mobile communication industry are also rising sharply. The hydrogen fuel cell backup power source with metal hydride hydrogen storage system proposed in this paper not only has the features of non-pollution, uninterrupted switching, high efficiency and long power supply time of conventional fuel cells but

also solves the problems of storage, transportation and safety of commonly used hydrogen fuel cells in use with metal hydride. The main conclusions of this paper are as follows:

- 1) Based on the cost prediction curve (Dear), it can be inferred that the hydrogen fuel cell backup power supply can be used around 2029 to gradually replace the existing lead-acid battery backup power supply system of large communication base stations.
- 2) At $H / H_{max} = 0.8$ o'clock, 291, 305 and 312 K conditions, the hydrogen absorption reaction rates were 0.29, 0.46 and 0.68 MPa, indicating that the hydrogen absorption reaction rate was accelerated with the increase in temperature.
- 3) The voltage response results show that the response time of AC blackout detection is about 5ms, which can meet the demand for an uninterrupted power supply to the equipment after a blackout.

In future research, there are still several difficulties that urgently need to be studied. The current design of numerous heat transfer structures is predominantly based on numerical simulation studies, which typically prioritize system performance. Considering the practical applications, it is important to evaluate the economics of different techniques to improve thermal conductivity, and there is still a deficiency in this area of research.

Funding:

This research was supported by the science and technology projects of China Southern Power Grid Company Limited (080000KK52210020).

References

- [1] Luta, D. N., & Raji, A. K. (2019). Renewable hydrogen-based energy system for supplying power to telecoms base station. *International journal of engineering research in Africa*, 43, 112-126.
- [2] Bahri, R., Keshavarzi, M. R., Zeynali, S., & Nasiri, N. (2023). Economic-environmental energy supply of mobile base stations in isolated nanogrids with smart plug-in electric vehicles and hydrogen energy storage system. *International journal of hydrogen energy*.
- [3] Sapru, K. (2017). Develop improved metal hydride technology for the storage of hydrogen. final technical report. Office of Scientific & Technical Information Technical Reports.
- [4] Morten, L., Mariem, M., Romain, M., Kateryna, P., & Michael, F. (2015). Development of hydrogen storage tank systems based on complex metal hydrides. *Materials*, 8(9), 5891-5921.
- [5] Capurso, G., Jepsen, J., Bellosta von Colbe, José M., Pistidda, C., Metz, O., & Yigit, D., et al. (2018). Engineering solutions in scale-up and tank design for metal hydrides. *Materials Science Forum*, 941, 2220-2225.
- [6] Lototskyy, M. V., Davids, M. W., Tolj, I., Klochko, Y. V., Sekhar, B. S., & Chidziva, S., et al. (2015). Metal hydride systems for hydrogen storage and supply for stationary and automotive low temperature pem fuel cell power modules. *International Journal of Hydrogen Energy*, 40(35), 11491-11497.
- [7] Gambini, M., Stilo, T., & Vellini, M. (2019). Hydrogen storage systems for fuel cells: comparison between high and low-temperature metal hydrides. *International Journal of Hydrogen Energy*, 44(29), 15118-15134.
- [8] B, H. Q. N. A., & A, B. S. (2021). Review of metal hydride hydrogen storage thermal management for use in the fuel cell systems. *International Journal of Hydrogen Energy*.

- [9] Schorn, F., Lohse, D., Samsun, R. C., Peters, R., & Stolten, D. (2021). The biogas-oxyfuel process as a carbon source for power-to-fuel synthesis: enhancing availability while reducing separation effort. *Journal of CO2 Utilization*, 45, 101410.
- [10] Li, C. (2018). Techno-economic study of off-grid hybrid photovoltaic/battery and photovoltaic/battery/fuel cell power systems in Kunming, China. *Energy Sources Part A Recovery Utilization and Environmental Effects*, 41(13-18), 1-17.
- [11] Mostafavi, S. A., Hajabdollahi, Z., & Ilinca, A. (2022). Multi-objective optimization of metal hydride hydrogen storage tank with phase change material. *Thermal Science and Engineering Progress*.
- [12] Sofía Peláez-Peláez, Colmenar-Santos, A., Clara Pérez-Molina, Rosales, A. E., & Rosales-Asensio, E. (2021). Techno-economic analysis of a heat and power combination system based on hybrid photovoltaic-fuel cell systems using hydrogen as an energy vector. *Energy*, 224(3), 120110.
- [13] Zhu, D., Ait-Amirat, Y., N'Diaye, A., & Djerdir, A. (2021). On-line state of charge estimation of embedded metal hydride hydrogen storage tank based on state classification. *Elsevier*.
- [14] Apostolou, D. (2021). Refuelling scenarios of a light urban fuel cell vehicle with metal hydride hydrogen storage. comparison with compressed hydrogen storage counterpart. *International Journal of Hydrogen Energy*(79), 46.
- [15] Garrigos, A., Blanes, J., & Lizdn, L. (2011). Non-isolated multiphase boost converter for a fuel cell with battery backup power system. *International Journal of Hydrogen Energy*, 36(10), 6259-6268.
- [16] Mansir, I. B., Hani, E. H. B., Farouk, N., Alarjani, A., Ayed, H., & Nguyen, D. D. (2022). Comparative transient simulation of a renewable energy system with hydrogen and battery energy storage for residential applications. *International Journal of Hydrogen Energy*.
- [17] Bedrunka, M., Bornemann, N., Steinebach, G., & Reith, D. (2022). A metal hydride system for a forklift: feasibility study on on-board chemical storage of hydrogen using numerical simulation. *International Journal of Hydrogen Energy*(24), 47.
- [18] Gonzatti, F., & Farret, F. A. (2017). Mathematical and experimental basis to model energy storage systems composed of electrolyzer, metal hydrides and fuel cells. *Energy Conversion & Management*, 132(jan.), 241-250.

About the Author

Hang Zhang was born in Luoyang, Henan, P.R. China, in 1990. He obtained a master's degree from Zhejiang University in China. He is currently working for Guangzhou Power Supply Bureau, Guangdong Power Grid Co., Ltd., his main research direction is electricity-hydrogen integrated energy system.

Jun Pan was born in Dongzhi, Anhui, P.R. China, in 1981. He obtained a master's degree from Shanghai Jiao Tong University in China. He is currently working for Guangzhou Power Supply Bureau, Guangdong Power Grid Co., Ltd., his main research direction is Hydrogen and fuel cells.

Jinyong Lei was born in Huizhou, Guangdong, P.R. China, in 1982. She obtained a doctor's degree from Zhejiang University in China. She is currently working for Guangzhou Power Supply Bureau, Guangdong Power Grid Co., Ltd., her main research direction is electricity-hydrogen integrated energy system.

Keying Feng was born in Guangzhou, Guangdong, P.R. China, in 1997. He obtained a master's degree from Tsinghua University in China. He is currently working for Guangzhou Power Supply Bureau, Guangdong Power Grid Co., Ltd., his main research direction is new energy materials.

Tianbao Ma was born in Jingmen, Hubei, P.R. China, in 1991. He obtained a Master's degree from HongKong University in China. He is currently working at Beijing Huasun Information Security Electronic Technology Co., Ltd. His main research direction is Hydrogen energy and Carbon neutralization field.